Weierstraß-Institut
für Angewandte Analysis und Stochastik

Leibniz-Institut im Forschungsverbund Berlin e. V.

Preprint ISSN 2198-5855

Pressure-robust approximation of the incompressible Navier–Stokes equations in a rotating frame of reference

Medine Demir[1], Volker John[1,2]

submitted: November 23, 2023

[1] Weierstraß-Institut
Mohrenstr. 39
10117 Berlin
Germany
E-Mail: medine.demir@wias-berlin.de
volker.john@wias-berlin.de

[2] Department of Mathematics and Computer Science
Freie Universität of Berlin
Arnimallee 6
14195 Berlin
Germany

No. 3058
Berlin 2023

2020 *Mathematics Subject Classification.* 65M15, 65M60, 76M10.

2010 *Physics and Astronomy Classification Scheme.* 47.10.ad, 47.11.Fg.

Key words and phrases. Navier–Stokes equations, rotating frame, Scott–Vogelius finite element method, pressure-robustness.

Edited by
Weierstraß-Institut für Angewandte Analysis und Stochastik (WIAS)
Leibniz-Institut im Forschungsverbund Berlin e. V.
Mohrenstraße 39
10117 Berlin
Germany

Fax: +49 30 20372-303
E-Mail: preprint@wias-berlin.de
World Wide Web: http://www.wias-berlin.de/

Pressure-robust approximation of the incompressible Navier–Stokes equations in a rotating frame of reference

Medine Demir, Volker John

Abstract

A pressure-robust space discretization of the incompressible Navier–Stokes equations in a rotating frame of reference is considered. The discretization employs divergence-free, H^1-conforming mixed finite element methods like Scott–Vogelius pairs. An error estimate for the velocity is derived that tracks the dependency of the error bound on the coefficients of the problem, in particular on the angular velocity. Numerical examples illustrate the theoretical results.

1 Introduction

This paper considers discretizations of the incompressible Navier–Stokes equations in a rotating frame of reference, which are given by

$$\begin{array}{rcll} \rho\partial_t \boldsymbol{u} - \mu\Delta\boldsymbol{u} + \rho(\boldsymbol{u}\cdot\nabla)\boldsymbol{u} + 2\rho\boldsymbol{\omega}\times\boldsymbol{u} + \nabla p &=& \boldsymbol{f} - \rho\boldsymbol{\omega}\times(\boldsymbol{\omega}\times\boldsymbol{r}) & \text{in } (0,T]\times\Omega, \\ \nabla\cdot\boldsymbol{u} &=& 0 & \text{in } (0,T]\times\Omega. \end{array} \tag{1}$$

Here, $\boldsymbol{u}$ $[\mathrm{m/s}]$ and p $[Pa]$ denote the unknown velocity field and the unknown pressure of the flow. The physical constants ρ $[\mathrm{kg/m^3}] > 0$, μ $[\mathrm{kg/ms}] > 0$, and $\boldsymbol{\omega}$ $[\mathrm{1/s}] \neq \boldsymbol{0}$ denote the density of the fluid, the dynamic viscosity of the fluid, and the angular velocity vector of the rotating frame of reference, respectively. These quantities are given. The kinematic viscosity is defined by $\nu = \mu/\rho$ $[\mathrm{m^2/s}]$. It is assumed that the axis of rotation meets the origin of the coordinate system. The position vector is denoted by $\boldsymbol{r}$ $[\mathrm{m}]$. Then, $2\rho\boldsymbol{\omega}\times\boldsymbol{u}$ and $\rho\boldsymbol{\omega}\times(\boldsymbol{\omega}\times\boldsymbol{r})$ model the Coriolis and the centripetal forces, respectively. Note that the centripetal force can be written as a gradient

$$\rho\boldsymbol{\omega}\times(\boldsymbol{\omega}\times\boldsymbol{r}) = -\nabla\phi_c \quad \text{with} \quad \phi_c = \frac{\rho}{2}\|\boldsymbol{\omega}\times\boldsymbol{r}\|_2^2,$$

where $\|\cdot\|_2$ denotes the Euclidean norm of a vector. The problem is posed in a bounded Lipschitz continuous domain $\Omega\subset\mathbb{R}^d$, $d\in\{2,3\}$, and in a finite time interval $(0,T]$. It will be considered with homogeneous Dirichlet boundary conditions

$$\boldsymbol{u}(t,\boldsymbol{x}) = \boldsymbol{0} \quad \text{in } [0,T]\times\partial\Omega,$$

where $\partial\Omega$ is the boundary of Ω. Finally, an initial condition

$$\boldsymbol{u}(0,\boldsymbol{x}) = \boldsymbol{u}_0(\boldsymbol{x}) \quad \text{in } \Omega$$

has to be prescribed.

Fluid equations in a rotating frame of reference have a broad class of important applications in meteorology and oceanography, especially in the large-scale flows considered in ocean and atmosphere, as well as many physical and industrial applications [1, 9]. The Coriolis and the centripetal forces, resulting from the rotation of the earth, play a crucial role in such systems. For such applications it may be required to solve the system in complex three-dimensional geometries. On one hand, one has to deal with the usual challenges in approximating problems of Navier–Stokes

DOI 10.20347/WIAS.PREPRINT.3058

type, which are nonlinearity, which require to satisfy or circumvent the discrete inf-sup condition, and which comprise dominating convection in the turbulent regime, see [17]. On the other hand, one has to properly handle the extra forces, namely the Coriolis and the centripetal forces, generating complicated fluid structures.

In recent years, the Navier–Stokes equations in a rotating frame have been investigated in a number of papers to contribute to the analysis and the accurate and efficient numerical simulation. For example, Refs. [12, 14, 15, 19] studied the global well-posedness of (1) with uniformly small initial data $\boldsymbol{u}_0$. An error analysis of a two step projection method was performed in [28]. In [33] one can find an error analysis of the incremental pressure-correction projection scheme. A discrete projection method was analyzed both theoretically and numerically for problem (1) in [32]. The main result of these projection methods is that the velocity is a first-order approximation and the pressure is an approximation of order 0.5. The analysis of an operator splitting method for the numerical solution of (1) can be found in [31].

It is well known that most of the classical inf-sup stable mixed methods for approximating the Navier–Stokes equations, like the H^1-conforming Taylor—Hood pairs of finite element spaces, suffer from poor mass conservation when the viscosity ν is small, e.g., see [18, 20, 25]. In addition, the pressure gradient balances forces of gradient type, which might be strong in practice. Numerical analysis reveals that classical methods, like Taylor–Hood pairs, introduce a pressure-dependent contribution in the velocity error bounds that is proportional to some inverse power of the viscosity, e.g., see [27, 18, 23, 24, 21, 4, 3]. Hence, these methods are optimally convergent but small velocity errors might not be achieved for complicated pressures and small viscosity coefficients. Several approaches have been proposed for improving the pressure-robustness of pairs of finite element spaces. One popular approach consists in applying grad-div stabilization [27, 4, 16, 26, 2]. Another approach is to use appropriate reconstructions of test functions [24, 23, 22]. Finally, it is possible to use pairs of spaces that lead to weakly divergence-free finite element solutions, like Scott–Vogelius pairs. However, this approach might come with additional requirements, like the use of barycentric-refined grids in case of Scott–Vogelius pairs, [30, 34].

In the literature, the Navier–Stokes equations with Coriolis force have been approximated most often by some projection method and using classical finite elements. To the best of the authors' knowledge, until now, no pressure-robust mixed method has been proposed and analyzed for these equations. This contribution studies the application of Scott–Vogelius pairs of finite element spaces to approximate the solution of (1). It will be shown that the method is stable and satisfies an energy equality. A velocity error estimate will be derived that is pressure-robust. The error bound does not depend explicitly on negative powers of the viscosity, but there is a dependency on the angular velocity. Numerical studies will support the analytic results.

The remainder of the paper is organized as follows. Section 2 provides some notations and mathematical preliminaries needed for the numerical analysis. In addition, the discretization with the Scott–Vogelius finite element method is introduced. Section 3 is devoted to the numerical analysis of the method. Numerical studies for verifying the analytic results are presented in Section 4. Finally, Section 5 provides a summary and an outlook.

2 Weak Formulation and Finite Element Discretization

Standard notations for Sobolev spaces and their norms will be used. In particular, the inner product in $L^2(\Omega)^d$, $d \geq 1$, is denoted by $(\cdot,\cdot)$ and the induced norm by $\|\cdot\|_0$. Sobolev spaces on Ω are denoted by $H^r(\Omega)$, $r \in \mathbb{R}$, $r > 0$, with the corresponding norm $\|\cdot\|_r$. Spaces for vector-valued functions are indicated with bold face symbols. Function spaces in spatio-temporal domains are denoted as usual with the time interval and the spatial function as arguments.

The space of weakly divergence-free functions is defined by

$$\boldsymbol{H}_{\mathrm{div}}(\Omega) = \Big\{\boldsymbol{\sigma} \in \boldsymbol{L}^2(\Omega) \,:\, \nabla\cdot\boldsymbol{\sigma} \in L^2(\Omega),\ -(\boldsymbol{\sigma},\nabla\psi) = 0 \,\forall\, \psi \in H^1(\Omega) \text{ and } \boldsymbol{\sigma}\cdot\boldsymbol{n} = 0\Big\},$$

with $\boldsymbol{n}$ being the unit outer normal at $\partial\Omega$. If a weakly divergence-free function is even from $\boldsymbol{H}_0^1(\Omega)$, then the corresponding subspace is denoted by

$$\boldsymbol{V}_{\mathrm{div}} = \Big\{\boldsymbol{v} \in \boldsymbol{H}_0^1(\Omega) \,:\, \nabla\cdot\boldsymbol{v} = 0\Big\}.$$

Then, a weak formulation of (1) with time-independent velocity test functions $\boldsymbol{v} \in \boldsymbol{V}_{\mathrm{div}}$ for computing the velocity $\boldsymbol{u} \in L^2\left(0,T;\boldsymbol{V}_{\mathrm{div}}\right) \cap L^\infty\left(0,T;\boldsymbol{H}_{\mathrm{div}}(\Omega)\right)$ is given by

$$\rho\left(\partial_t\boldsymbol{u},\boldsymbol{v}\right) + \mu\left(\nabla\boldsymbol{u},\nabla\boldsymbol{v}\right) + \rho\left((\boldsymbol{u}\cdot\nabla)\boldsymbol{u},\boldsymbol{v}\right) + 2\left(\boldsymbol{\omega}\times\boldsymbol{u},\boldsymbol{v}\right) = \langle\boldsymbol{f},\boldsymbol{v}\rangle_{\boldsymbol{H}^{-1},\boldsymbol{H}_0^1} \tag{2}$$

for all $\boldsymbol{v} \in \boldsymbol{V}_{\mathrm{div}}$, where $\boldsymbol{f} \in L^2\left(0,T;\boldsymbol{H}^{-1}(\Omega)\right)$ is assumed and the symbol for the right-hand side denotes the dual pairing. The pressure and the centripetal force do not occur in this weak formulation because they are gradients that are tested with a weakly divergence-free function. The initial value is $\boldsymbol{u}_0(\boldsymbol{x}) \in \boldsymbol{H}_{\mathrm{div}}(\Omega)$.

Let $\{\mathcal{T}_h\}$, $h > 0$, be a family of admissible and quasi-uniform triangulations of Ω. For the discretization in space, the Scott–Vogelius pair of finite element spaces $(\boldsymbol{V}_h, Q_h) = (\boldsymbol{P}_r, P_{r-1}^{\mathrm{disc}})$, proposed in [30], for approximating velocity and pressure will be considered. This pair is known to fulfil the discrete inf-sup condition

$$\inf_{0\neq q_h\in Q_h}\ \sup_{0\neq\boldsymbol{v}_h\in\boldsymbol{V}_h} \frac{(\nabla\cdot\boldsymbol{v}_h,\, q_h)}{\|\nabla\boldsymbol{v}_h\|_0\|q_h\|_0} = \beta_h > 0, \tag{3}$$

independently of the mesh width under certain restrictions on the mesh and polynomial degree, e.g.,

- in $2d$, if $r \geq 4$ and the mesh has no singular vertices, [30],
- when $r \geq d$ and the mesh is a barycentric refinement of a regular mesh, [34, 29].

This paper considers such situations, so that (3) holds.

An attractive property of the Scott–Vogelius element is that the discrete mass conservation enforced with

$$(\nabla\cdot\boldsymbol{v}_h, q_h) = 0 \quad \forall\, q_h \in Q_h,$$

implies even weak mass conservation, since $\|\nabla\cdot\boldsymbol{v}_h\|_0 = 0$ by the special choice of $q_h = \nabla\cdot\boldsymbol{v}_h$, which is possible due to $\nabla\cdot\boldsymbol{V}_h \subset Q_h$. Hence the discretely divergence-free subspace of $\boldsymbol{V}_h$ can be characterized as follows

$$\begin{aligned}\boldsymbol{V}_{h,\mathrm{div}} &= \{\boldsymbol{v}_h \in \boldsymbol{V}_h \,:\, (\nabla\cdot\boldsymbol{v}_h, q_h) = 0,\ \forall\, q_h \in Q_h\} \\ &= \{\boldsymbol{v}_h \in \boldsymbol{V}_h \,:\, \|\nabla\cdot\boldsymbol{v}_h\|_0 = 0\}.\end{aligned}$$

Note that the elements of $\boldsymbol{V}_{h,\mathrm{div}}$ are weakly divergence-free and hence $\boldsymbol{V}_{h,\mathrm{div}} \subset \boldsymbol{H}_{\mathrm{div}}(\Omega)$.

A modified Stokes projection $\boldsymbol{s}_h \,:\, \boldsymbol{V} \to \boldsymbol{V}_{h,\mathrm{div}}$ is considered for the error analysis of the velocity, see [8], satisfying

$$(\nabla\boldsymbol{s}_h, \nabla\boldsymbol{v}_h) = (\nabla\boldsymbol{u}, \nabla\boldsymbol{v}_h) \quad \forall\, \boldsymbol{v}_h \in \boldsymbol{V}_{h,\mathrm{div}}. \tag{4}$$

The following bound holds for $m \in \{0,1\}$, compare [8],

$$\|\boldsymbol{u}_h - \boldsymbol{s}_h\|_m \leq Ch^{r+1-m}\|\boldsymbol{u}\|_{r+1} \quad \forall\, \boldsymbol{u} \in \boldsymbol{V} \cap H^{r+1}(\Omega)^d. \tag{5}$$

In addition, the following bounds are valid, see [11, (3.32)], [7, (21)], [5],

$$\|\boldsymbol{s}_h\|_{L^\infty} \leq C(\|\boldsymbol{u}\|_{d-2}\|\boldsymbol{u}\|_2)^{1/2}, \quad \|\nabla \boldsymbol{s}_h\|_{L^\infty} \leq C\|\nabla \boldsymbol{u}\|_{L^\infty}. \tag{6}$$

If $\partial_t \boldsymbol{u}$ is sufficiently regular, a modified Stokes projection of the form (4) can be defined for $\partial_t \boldsymbol{u}$ and error bounds of the form (5) can be derived for $\partial_t(\boldsymbol{u} - \boldsymbol{s}_h)$.

In the semi-discrete problem (continuous-in-time problem), the centripetal force will be added to the pressure to define a modified discrete pressure, which is denoted for simplicity also by p_h. Let $(\boldsymbol{V}_h, Q_h)$ be a pair of Scott–Vogelius finite element spaces satisfying (3), the semi-discrete problem reads as follows: find $\boldsymbol{u}_h : (0,T] \to \boldsymbol{V}_h$ and $p_h : (0,T) \to Q_h$ such that for all $(\boldsymbol{v}_h, q_h) \in (\boldsymbol{V}_h, Q_h)$ it holds

$$\begin{aligned} \rho\,(\partial_t \boldsymbol{u}_h, \boldsymbol{v}_h\,) + \mu\,(\nabla \boldsymbol{u}_h, \nabla \boldsymbol{v}_h) + \rho\,((\boldsymbol{u}_h \cdot \nabla)\boldsymbol{u}_h, \boldsymbol{v}_h) & \\ + \rho\,(2\boldsymbol{\omega} \times \boldsymbol{u}_h, \boldsymbol{v}_h) - (\nabla \cdot \boldsymbol{v}_h, p_h) &= \langle \boldsymbol{f}, \boldsymbol{v}_h \rangle_{\boldsymbol{H}^{-1}, \boldsymbol{H}_0^1}, \\ (\nabla \cdot \boldsymbol{u}_h, q_h) &= 0, \end{aligned} \tag{7}$$

with an initial velocity $\boldsymbol{u}_h(0, \boldsymbol{x})$, which is an appropriate approximation of $\boldsymbol{u}_0(\boldsymbol{x})$ in $\boldsymbol{V}_h$. Note that

$$((\boldsymbol{u}_h \cdot \nabla)\boldsymbol{v}_h, \boldsymbol{v}_h) = 0 \quad \forall\, \boldsymbol{v}_h \in \boldsymbol{V}_h, \tag{8}$$

since $\boldsymbol{u}_h \in \boldsymbol{V}_{h,\mathrm{div}} \subset \boldsymbol{V}_{\mathrm{div}}$. In addition, since the vector $\boldsymbol{\omega} \times \boldsymbol{v}_h$ is perpendicular to $\boldsymbol{v}_h$, it is

$$(2\boldsymbol{\omega} \times \boldsymbol{v}_h, \boldsymbol{v}_h) = 0 \quad \forall\, \boldsymbol{v}_h \in \boldsymbol{V}_h. \tag{9}$$

3 Numerical Analysis

This section presents the analysis of method (7): consistency, energy equality, stability, and a velocity error estimate.

Lemma 3.1 (Consistency) *For any velocity solution $\boldsymbol{u}$ of* (2) *satisfying $\boldsymbol{u} \in \boldsymbol{V}_h$ for all $t > 0$ and $\boldsymbol{u}_0(\boldsymbol{x}) = \boldsymbol{u}_h(0, \boldsymbol{x})$, it holds that $\boldsymbol{u}_h(t) = \boldsymbol{u}(t)$ for all $t \in [0,T]$.*

Proof: By assumption both problems (2) and (7) have the same initial condition.

A velocity field is a solution of the discrete problem if and only if it satisfies the discrete initial condition and it holds for all test functions from $\boldsymbol{V}_{h,\mathrm{div}}$

$$\begin{aligned} \rho\,(\partial_t \boldsymbol{u}_h, \boldsymbol{v}_h\,) + \mu\,(\nabla \boldsymbol{u}_h, \nabla \boldsymbol{v}_h) + \rho\,((\boldsymbol{u}_h \cdot \nabla)\boldsymbol{u}_h, \boldsymbol{v}_h) & \\ + \rho\,(2\boldsymbol{\omega} \times \boldsymbol{u}_h, \boldsymbol{v}_h) &= \langle \boldsymbol{f}, \boldsymbol{v}_h \rangle_{\boldsymbol{H}^{-1}, \boldsymbol{H}_0^1}. \end{aligned}$$

Since for the Scott–Vogelius pair of spaces $\boldsymbol{V}_{h,\mathrm{div}} \subset \boldsymbol{V}_{\mathrm{div}}$, these test functions can be used also in the continuous problem (2), showing that $\boldsymbol{u}$ satisfies the same equation. ■

Lemma 3.2 (Energy equality and stability) *For any velocity solution $\boldsymbol{u}_h \in \boldsymbol{V}_h$ of the spatially discretized problem* (7) *holds, for all t $\in (0,T]$, the energy equality*

$$\frac{1}{2}\|\boldsymbol{u}_h(t)\|_0^2 + \mu \int_0^t \|\nabla \boldsymbol{u}_h(s)\|_0^2 \,\mathrm{d}s = \frac{1}{2}\|\boldsymbol{u}_h(0,\cdot)\|_0^2 + \int_0^t \langle \boldsymbol{f}(s), \boldsymbol{u}_h(s) \rangle_{\boldsymbol{H}^{-1}, \boldsymbol{H}_0^1} \,\mathrm{d}s$$

and the a priori estimate (stability estimate)

$$\|\boldsymbol{u}_h(t)\|_0^2 + \mu \int_0^t \|\nabla \boldsymbol{u}_h(s)\|_0^2 \,\mathrm{d}s \leq \|\boldsymbol{u}_h(0)\|_0^2 + \mu^{-1} \int_0^t \|\boldsymbol{f}(s)\|_{\boldsymbol{H}^{-1}}^2 \,\mathrm{d}s.$$

Proof: Testing (7) by $\boldsymbol{v}_h = \boldsymbol{u}_h(s) \in \boldsymbol{V}_{h,\mathrm{div}}$, with fixed $s \in (0, T]$, and using the definition of the kinematic viscosity, (8), and (9) yields

$$\frac{1}{2}\frac{d}{dt}\|\boldsymbol{u}_h(s)\|_0^2 + \mu\|\nabla\boldsymbol{u}_h(s)\|_0^2 = \langle \boldsymbol{f}(s), \boldsymbol{u}_h(s)\rangle_{\boldsymbol{H}^{-1},\boldsymbol{H}_0^1}. \tag{10}$$

Integrating over the time interval $(0, t) \subset (0, T]$ gives the energy equality.

Applying the Cauchy–Schwarz and the Young inequalities on the right-hand side of (10) leads to

$$\begin{aligned}\frac{1}{2}\frac{d}{dt}\|\boldsymbol{u}_h(s)\|_0^2 + \mu\|\nabla\boldsymbol{u}_h(s)\|_0^2 &\leq \|\boldsymbol{f}(s)\|_{\boldsymbol{H}^{-1}}\|\nabla\boldsymbol{u}_h(s)\|_0 \\ &\leq \frac{1}{2\mu}\|\boldsymbol{f}(s)\|_{\boldsymbol{H}^{-1}}^2 + \frac{\mu}{2}\|\nabla\boldsymbol{u}_h(s)\|_0^2.\end{aligned}$$

The stability estimate is obtained by integrating the inequality over $(0, t) \subset (0, T]$. ■

We proceed to present an error analysis for the velocity solution of (7).

Theorem 3.1 (Velocity error estimate) *Assume for the solution of* (2) *that*

$$\begin{aligned}\boldsymbol{u} \in\ & L^2(0, T; \boldsymbol{V}_{\mathrm{div}}) \cap L^2\left(0, T; \boldsymbol{H}^{r+1}(\Omega)\right) \cap L^\infty(0, T; \boldsymbol{H}_{\mathrm{div}}(\Omega)) \\ & \cap L^\infty\left(0, T; \boldsymbol{H}^{\max\{2,r\}}(\Omega)\right) \cap L^1\left(0, T; \boldsymbol{W}^{1,\infty}(\Omega)\right)\end{aligned}$$

and assume that $\boldsymbol{\omega} \in L^\infty(0, T; \boldsymbol{L}^\infty(\Omega))$. Let $\boldsymbol{u}_h$ be the velocity solution of (7)*. Then, the following error estimate holds*

$$\begin{aligned}&\|(\boldsymbol{u} - \boldsymbol{u}_h)(t)\|_0^2 + \nu\|\nabla(\boldsymbol{u} - \boldsymbol{u}_h)\|_{L^2((0,t);L^2)}^2 \\ &\leq Ch^{2r}\left(\|\boldsymbol{u}(t)\|_{L^\infty((0,t);H^r)}^2 + \nu\|\nabla\boldsymbol{u}\|_{L^2((0,t);H^r)}^2 + \exp(L(T, \boldsymbol{u}))\, M(T, \boldsymbol{u}, \boldsymbol{\omega})\right) \\ &\quad +2\exp(L(T, \boldsymbol{u}))\,\|\boldsymbol{u}_h(0) - \boldsymbol{s}_h(0)\|_0^2,\end{aligned} \tag{11}$$

for all $t \in (0, T]$ with

$$L(T, \boldsymbol{u}) = 2\int_0^T (\|\nabla\boldsymbol{u}\|_{L^\infty} + 1)\ \mathrm{d}s, \tag{12}$$

and

$$M(T, \boldsymbol{u}, \boldsymbol{\omega}) = \int_0^T \left(\|\boldsymbol{u}\|_1\|\boldsymbol{u}\|_2\|\boldsymbol{u}\|_{r+1}^2 + \|\partial_t\boldsymbol{u}\|_r^2 + \|\boldsymbol{\omega}\|_{L^\infty}^2\|\boldsymbol{u}\|_r^2\right)\ \mathrm{d}s. \tag{13}$$

The constant in (11) *does not blow up as ν tends to zero.*

Proof: The proof follows the proof of [10, Theorem 4.7]. The error is split into

$$\boldsymbol{e} = \boldsymbol{u} - \boldsymbol{u}_h = (\boldsymbol{u} - \boldsymbol{s}_h) - (\boldsymbol{u}_h - \boldsymbol{s}_h) = \boldsymbol{\eta} - \boldsymbol{\phi}_h,$$

where $\boldsymbol{s}_h$ is the Stokes projection defined in (4). Hence, it is $\boldsymbol{\phi}_h \in \boldsymbol{V}_{h,\mathrm{div}}$. Then, subtracting (7) from (2) and using (4) leads to the error equation

$$\begin{aligned}\rho(\partial_t\boldsymbol{\phi}_h, \boldsymbol{v}_h) + \mu(\nabla\boldsymbol{\phi}_h, \nabla\boldsymbol{v}_h) + \rho((\boldsymbol{u}_h\cdot\nabla)\boldsymbol{u}_h, \boldsymbol{v}_h) - \rho((\boldsymbol{s}_h\cdot\nabla)\boldsymbol{s}_h, \boldsymbol{v}_h)& \\ +\rho(2\boldsymbol{\omega}\times\boldsymbol{\phi}_h, \boldsymbol{v}_h) \quad = \quad \rho(\partial_t\boldsymbol{\eta}, \boldsymbol{v}_h) + \rho((\boldsymbol{u}\cdot\nabla)\boldsymbol{u}, \boldsymbol{v}_h) - \rho((\boldsymbol{s}_h\cdot\nabla)\boldsymbol{s}_h, \boldsymbol{v}_h)& \\ +\rho(2\boldsymbol{\omega}\times\boldsymbol{\eta}, \boldsymbol{v}_h) \quad \forall\, \boldsymbol{v}_h \in \boldsymbol{V}_{h,\mathrm{div}}.&\end{aligned}$$

Taking $\boldsymbol{v}_h = \boldsymbol{\phi}_h$ and using (9) yields

$$\frac{\rho}{2}\frac{d}{dt}\|\boldsymbol{\phi}_h\|_0^2 + \mu\|\nabla\boldsymbol{\phi}_h\|_0^2 \leq \rho\,|((\boldsymbol{u}_h\cdot\nabla)\boldsymbol{u}_h, \boldsymbol{\phi}_h) - ((\boldsymbol{s}_h\cdot\nabla)\boldsymbol{s}_h, \boldsymbol{\phi}_h)|$$

$$
\begin{aligned}
&+\rho\left|((\boldsymbol{u}\cdot\nabla)\boldsymbol{u},\boldsymbol{\phi}_h)-\rho\left((\boldsymbol{s}_h\cdot\nabla)\boldsymbol{s}_h,\boldsymbol{\phi}_h\right)\right| \\
&+\rho\left|(\partial_t\boldsymbol{\eta},\boldsymbol{\phi}_h)\right|+\rho\left|(2\boldsymbol{\omega}\times\boldsymbol{\eta},\boldsymbol{\phi}_h)\right|. \qquad (14)
\end{aligned}
$$

The first term on the right-hand side of (14) is bounded by adding and subtracting $(\boldsymbol{u}_h\cdot\nabla)\boldsymbol{s}_h,\boldsymbol{\phi}_h)$, applying the triangle inequality, using the skew-symmetric property of the nonlinear term for weakly divergence-free functions (8), and finally Hölder's inequality

$$
\begin{aligned}
&\rho|\left((\boldsymbol{u}_h\cdot\nabla)\boldsymbol{u}_h,\boldsymbol{\phi}_h\right)-\left((\boldsymbol{s}_h\cdot\nabla)\boldsymbol{s}_h,\boldsymbol{\phi}_h\right)| \\
&\quad\le\ \rho|\left((\boldsymbol{u}_h\cdot\nabla)\boldsymbol{\phi}_h,\boldsymbol{\phi}_h\right)|+\rho|\left((\boldsymbol{\phi}_h\cdot\nabla)\boldsymbol{s}_h,\boldsymbol{\phi}_h\right)|=\rho|\left((\boldsymbol{\phi}_h\cdot\nabla)\boldsymbol{s}_h,\boldsymbol{\phi}_h\right)| \\
&\quad\le\ \rho\|\nabla\boldsymbol{s}_h\|_{L^\infty}\|\boldsymbol{\phi}_h\|_0^2.
\end{aligned}
$$

For bounding the second term on the right-hand side of (14), $((\boldsymbol{s}_h\cdot\nabla)\boldsymbol{u},\boldsymbol{\phi}_h)$ is added and subtracted, Hölder's inequality, Sobolev embeddings, a Sobolev interpolation, (6), and (5) are used to obtain

$$
\begin{aligned}
&\rho\left|((\boldsymbol{u}\cdot\nabla)\boldsymbol{u},\boldsymbol{\phi}_h)-\rho\left((\boldsymbol{s}_h\cdot\nabla)\boldsymbol{s}_h,\boldsymbol{\phi}_h\right)\right| \\
&\quad\le\ \rho\left|((\boldsymbol{\eta}\cdot\nabla)\boldsymbol{u},\boldsymbol{\phi}_h)\right|+\left|(\boldsymbol{s}_h\cdot\nabla)\boldsymbol{\eta},\boldsymbol{\phi}_h)\right| \\
&\quad\le\ \rho\|\boldsymbol{\eta}\|_{L^6}\|\nabla\boldsymbol{u}\|_{L^3}\|\boldsymbol{\phi}_h\|_0+\|\boldsymbol{s}_h\|_{L^\infty}\|\nabla\boldsymbol{\eta}\|_0\|\boldsymbol{\phi}_h\|_0 \\
&\quad\le\ C\rho\left(\|\nabla\boldsymbol{u}\|_{1/2}+\|\boldsymbol{s}_h\|_{L^\infty}\right)\|\boldsymbol{\eta}\|_1\|\boldsymbol{\phi}_h\|_0 \\
&\quad\le\ C\rho\left(\left(\|\boldsymbol{u}\|_1\|\boldsymbol{u}\|_2\right)^{1/2}+\|\boldsymbol{s}_h\|_{L^\infty}\right)\|\boldsymbol{\eta}\|_1\|\boldsymbol{\phi}_h\|_0 \\
&\quad\le\ C\rho h^r\left(\|\boldsymbol{u}\|_1\|\boldsymbol{u}\|_2\right)^{1/2}\|\boldsymbol{u}\|_{r+1}\|\boldsymbol{\phi}_h\|_0.
\end{aligned}
$$

The third term on the right-hand side of (14) is estimated by applying the Cauchy–Schwarz inequality and (5) for the temporal derivative

$$
\rho\left|(\partial_t\boldsymbol{\eta},\boldsymbol{\phi}_h)\right|\le\rho\|\partial_t\boldsymbol{\eta}\|_0\|\boldsymbol{\phi}_h\|_0\le C\rho h^r\|\partial_t\boldsymbol{u}\|_r\|\boldsymbol{\phi}_h\|_0.
$$

And the last term is estimated similarly

$$
\rho\left|(2\boldsymbol{\omega}\times\boldsymbol{\eta},\boldsymbol{\phi}_h)\right|\le 2\rho\|\boldsymbol{\omega}\|_{L^\infty}\|\boldsymbol{\eta}\|_0\|\boldsymbol{\phi}_h\|_0\le C\rho h^r\|\boldsymbol{\omega}\|_{L^\infty}\|\boldsymbol{u}\|_r\|\boldsymbol{\phi}_h\|_0.
$$

Inserting all estimates, applying Young's inequality, and multiplying with $2/\rho$ gives

$$
\begin{aligned}
\frac{d}{dt}\|\boldsymbol{\phi}_h\|_0^2+2\nu\|\nabla\boldsymbol{\phi}_h\|_0^2\ \le\ & Ch^{2r}\left(\|\boldsymbol{u}\|_1\|\boldsymbol{u}\|_2\|\boldsymbol{u}\|_{r+1}^2+\|\partial_t\boldsymbol{u}\|_r^2+\|\boldsymbol{\omega}\|_{L^\infty}^2\|\boldsymbol{u}\|_r^2\right) \\
&+2\left(\|\nabla\boldsymbol{s}_h\|_{L^\infty}+1\right)\|\boldsymbol{\phi}_h\|_0^2.
\end{aligned}
$$

By the regularity assumptions, all terms in the parentheses are in $L^1(0,T)$, so that Gronwall's lemma can be applied. One obtains for any $t\in(0,T]$

$$
\begin{aligned}
&\|\boldsymbol{\phi}_h(t)\|_0^2+2\nu\|\nabla\boldsymbol{\phi}_h\|_{L^2((0,t);L^2)}^2 \\
&\quad\le\ \exp\left(L(T,\boldsymbol{u})\right)\|\boldsymbol{\phi}_h(0)\|_0^2+Ch^{2r}\exp\left(L(T,\boldsymbol{u})\right)M(T,\boldsymbol{u},\boldsymbol{\omega}),
\end{aligned}
$$

where $L(T,\boldsymbol{u})$ and $M(T,\boldsymbol{u},\boldsymbol{\omega})$ are defined in (12) and (13), respectively.

The application of the triangle inequality concludes the proof. ■

In contrast to the robustness of the error (11) with respect to the viscosity, the bound blows up if the angular velocity increases. It can be seen that the predicted blow-up is not exponential but linear for one term of the error bound (note that the square of the error is considered in (11)).

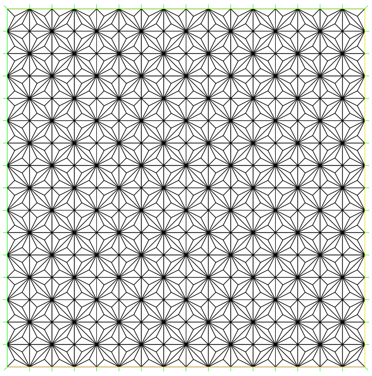

Figure 1: The domain of the numerical problem with a barycentric-refined grid.

4 Numerical Studies

This section presents a few numerical studies to verify the theoretical results for method (7). For this purpose, we consider (1) with the prescribed solution

$$\begin{aligned} \boldsymbol{u}_1 &= \pi \sin(t)\sin(2\pi y)\sin^2(\pi x), \\ \boldsymbol{u}_2 &= -\pi \sin(t)\sin(2\pi x)\sin^2(\pi y), \\ p &= \sin(t)\cos(\pi x)\sin(\pi y). \end{aligned} \tag{15}$$

Simulations are performed in the unit square $\Omega = (0,1)^2$ and with the final time $T = 1$. The external force $\boldsymbol{f}$, the Dirichlet boundary condition, and the initial condition were determined by (15). We considered $\rho = 1\ {}^{\mathrm{kg}}/_{\mathrm{m}^3}$ and simulations with different values of μ and $\boldsymbol{\omega}$ were performed. Note that in two dimensions the angular velocity is $\boldsymbol{\omega} = \omega \boldsymbol{e}_z$, where $\boldsymbol{e}_z$ is the Cartesian unit vector in z-direction. As temporal discretization, the second order linearly extrapolated backward differentiation formula (BDF2LE), i.e., replacing the first factor in the convective term $\boldsymbol{u}_h^{n+1} \cdot \nabla \boldsymbol{u}_h^{n+1}$ with the extrapolation $(2\boldsymbol{u}_h^n - \boldsymbol{u}_h^{n-1})$, is used. In order that the temporal discretization error is negligible, the very small time step $\Delta t = 0.0001$ was applied, hence the number of time steps is $N = 10000$. As spatial discretization, the Scott–Vogelius pair $(P_2, P_1^{\mathrm{disc}})$, i.e., $r = 2$, defined on barycentric refinements was used. The simulations are performed with the finite element software package FreeFem++ [13], where the UMFPACK sparse direct linear solver [6] was applied for solving the linear systems of equations.

We computed numerical solutions on successively refined meshes and refinements with $h \in \{1/8, 1/16, 1/32, 1/64\}$ were considered. An example of a barycentric-refined mesh can be seen in Figure 1.

The studied errors are given by

$$\|\boldsymbol{u} - \boldsymbol{u}_h\|_{L^\infty(L^2)} = \max_{t^n \in [0,T]} \|(\mathbf{u} - \mathbf{u}_h)(t^n)\|_{L^2}, \tag{16}$$

$$\mu^{1/2}\|\nabla(\mathbf{u} - \mathbf{u}_h)\|_{L^2([0,1];L^2)} = \left(\mu \sum_{n=1}^{N} \Delta t \|\nabla(\mathbf{u}(t^n) - \mathbf{u}_h^n)\|_{L^2}^2\right)^{1/2}, \tag{17}$$

and the square root of the term on the left-hand side of (11) (which is abbreviated with 'l.h.s. of error estimate').

We first performed a study for varying viscosity $\mu \in \{1, 10^2, 10^4, 10^6\}$ with fixed angular velocity $\omega = 1$, see Figure 2. This study aimed to check the robustness of the errors with respect to viscosity. The robustness of the error on the left-hand side of (11) for small viscosity coefficients as well as the predicted second order of convergence of this term can be clearly observed. With

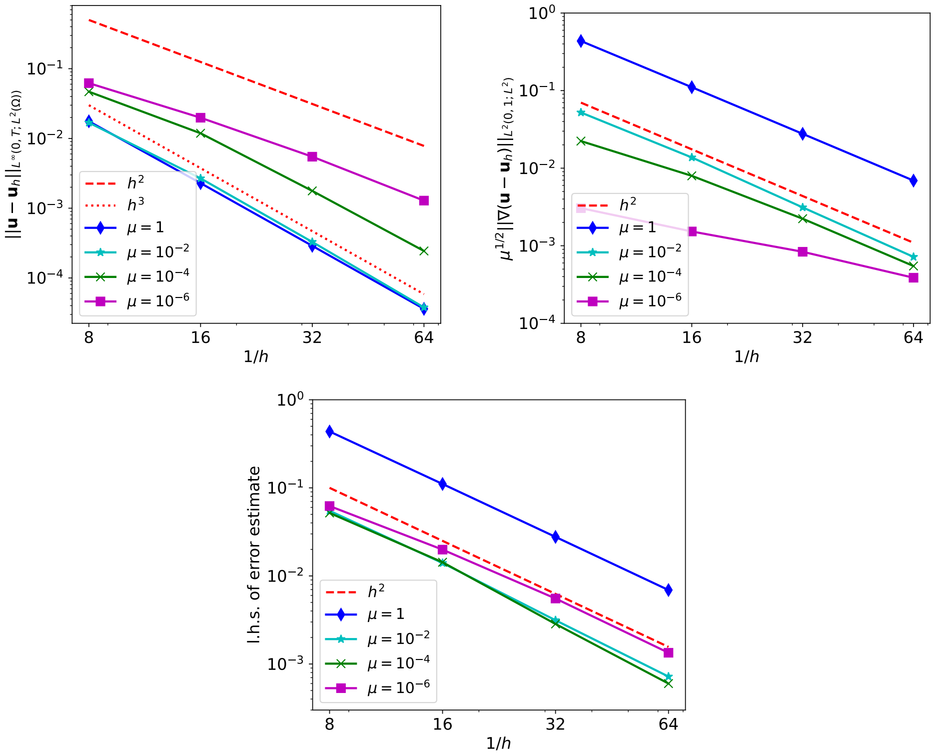

Figure 2: Velocity errors for varying viscosity μ and fixed $\omega = 1$. The bottom picture is for the square root of the left-hand side of error estimate (11).

respect to the error in $L^\infty(L^2)$ defined in (16), a small increase can be observed if the viscosity decreases, but not a blow up. Apart of the smallest viscosity coefficient, third order convergence can be already seen. The error given in (17) is robust. For all but the smallest viscosity coefficient, the second order convergence is already visible.

The second study was for fixed $\mu = 1$ and varying $\omega \in \{1, 10^2, 10^4, 10^6\}$. In this case the error bound (11) predicts a linear dependency on the angular velocity. However, the considered example seems not to be a worst case, as considered in the error analysis, or the error bound is dominated by a term that does not depend on ω since the angular velocity does not possess much impact on the errors, compare Figure 3. The expected orders of convergence can be observed.

5 Conclusion

This paper studied a finite element discretization of the Navier–Stokes equations in a rotating frame of reference. To this end, the classical Scott–Vogelius pairs of finite element spaces were considered, which lead to weakly divergence-free velocity solutions. As main result, it was shown that the velocity error in a standard norm can be bounded with the expected order of convergence and in a pressure-robust way. The error bound is also convection-robust in the sense that it does not explicitly contain inverse powers of the viscosity. One term of the error bound depends linearly on the angular velocity. The theoretical results were validated with numerical studies.

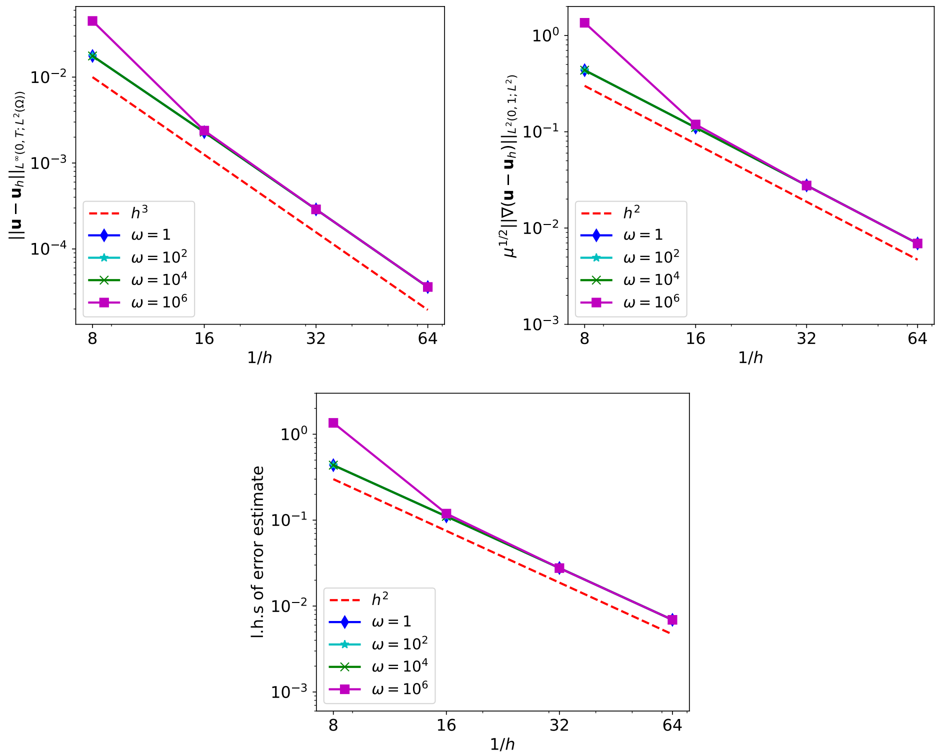

Figure 3: Velocity errors for fixed $\mu = 1$ and varying ω. The bottom picture is for the square root of the left-hand side of error estimate (11).

References

[1] B. Y. Ballal and R. S. Rivlin. Flow of a Newtonian fluid between eccentric rotating cylinders: inertial effects. *Arch. Rational Mech. Anal.*, 62(3):237–294, 1976.

[2] M. Braack, E. Burman, V. John, and G. Lube. Stabilized finite element methods for the generalized Oseen problem. *Comput. Methods Appl. Mech. Engrg.*, 196(4-6):853–866, 2007.

[3] C. Brennecke, A. Linke, C. Merdon, and J. Schöberl. Optimal and pressure-independent L^2 velocity error estimates for a modified Crouzeix-Raviart Stokes element with BDM reconstructions. *J. Comput. Math.*, 33(2):191–208, 2015.

[4] Michael A. Case, Vincent J. Ervin, Alexander Linke, and Leo G. Rebholz. A connection between Scott-Vogelius and grad-div stabilized Taylor-Hood FE approximations of the Navier-Stokes equations. *SIAM J. Numer. Anal.*, 49(4):1461–1481, 2011.

[5] Hongsen Chen. Pointwise error estimates for finite element solutions of the Stokes problem. *SIAM J. Numer. Anal.*, 44(1):1–28, 2006.

[6] Timothy A. Davis. Algorithm 832: UMFPACK V4.3—an unsymmetric-pattern multifrontal method. *ACM Trans. Math. Software*, 30(2):196–199, 2004.

[7] Javier de Frutos, Bosco Garcí a Archilla, Volker John, and Julia Novo. Analysis of the grad-div stabilization for the time-dependent Navier-Stokes equations with inf-sup stable finite elements. *Adv. Comput. Math.*, 44(1):195–225, 2018.

[8] Javier de Frutos, Bosco García-Archilla, Volker John, and Julia Novo. Grad-div stabilization for the evolutionary Oseen problem with inf-sup stable finite elements. *J. Sci. Comput.*, 66(3):991–1024, 2016.

[9] Schunxin Feng, Qibing Li, and Song Fu. On the orbital motion of a rotating inner cylinder in annular flow. *Int. J. Numer. Methods Fluids*, 54:155–173, 2007.

[10] Bosco García-Archilla, Volker John, and Julia Novo. On the convergence order of the finite element error in the kinetic energy for high Reynolds number incompressible flows. *Comput. Methods Appl. Mech. Engrg.*, 385:Paper No. 114032, 54, 2021.

[11] Bosco García-Archilla, Julia Novo, and Edriss S. Titi. Uniform in time error estimates for a finite element method applied to a downscaling data assimilation algorithm for the Navier-Stokes equations. *SIAM J. Numer. Anal.*, 58(1):410–429, 2020.

[12] Yoshikazu Giga, Katsuya Inui, Alex Mahalov, and Jürgen Saal. Uniform global solvability of the rotating Navier-Stokes equations for nondecaying initial data. *Indiana Univ. Math. J.*, 57(6):2775–2791, 2008.

[13] F. Hecht. New development in freefem++. *J. Numer. Math.*, 20(3-4):251–265, 2012.

[14] Matthias Hieber and Yoshihiro Shibata. The Fujita-Kato approach to the Navier-Stokes equations in the rotational framework. *Math. Z.*, 265(2):481–491, 2010.

[15] Tsukasa Iwabuchi and Ryo Takada. Global well-posedness and ill-posedness for the Navier-Stokes equations with the Coriolis force in function spaces of Besov type. *J. Funct. Anal.*, 267(5):1321–1337, 2014.

[16] Eleanor W. Jenkins, Volker John, Alexander Linke, and Leo G. Rebholz. On the parameter choice in grad-div stabilization for the Stokes equations. *Adv. Comput. Math.*, 40(2):491–516, 2014.

[17] Volker John. *Finite Element Methods for Incompressible Flow Problems*. Springer Series in Computational Mathematics Volume 51, Berlin, 2016.

[18] Volker John, Alexander Linke, Christian Merdon, Michael Neilan, and Leo G. Rebholz. On the divergence constraint in mixed finite element methods for incompressible flows. *SIAM Rev.*, 59(3):492–544, 2017.

[19] Paweł Konieczny and Tsuyoshi Yoneda. On dispersive effect of the Coriolis force for the stationary Navier-Stokes equations. *J. Differential Equations*, 250(10):3859–3873, 2011.

[20] A. Linke and C. Merdon. Pressure-robustness and discrete Helmholtz projectors in mixed finite element methods for the incompressible Navier-Stokes equations. *Comput. Methods Appl. Mech. Engrg.*, 311:304–326, 2016.

[21] A. Linke, C. Merdon, and W. Wollner. Optimal L^2 velocity error estimate for a modified pressure-robust Crouzeix-Raviart Stokes element. *IMA J. Numer. Anal.*, 37(1):354–374, 2017.

[22] Alexander Linke. A divergence-free velocity reconstruction for incompressible flows. *C. R. Math. Acad. Sci. Paris*, 350(17-18):837–840, 2012.

[23] Alexander Linke. On the role of the Helmholtz decomposition in mixed methods for incompressible flows and a new variational crime. *Comput. Methods Appl. Mech. Engrg.*, 268:782–800, 2014.

[24] Alexander Linke, Gunar Matthies, and Lutz Tobiska. Robust arbitrary order mixed finite element methods for the incompressible Stokes equations with pressure independent velocity errors. *ESAIM Math. Model. Numer. Anal.*, 50(1):289–309, 2016.

[25] Alexander Linke and Leo G. Rebholz. Pressure-induced locking in mixed methods for time-dependent (Navier-)Stokes equations. *J. Comput. Phys.*, 388:350–356, 2019.

[26] Maxim Olshanskii, Gert Lube, Timo Heister, and Johannes Löwe. Grad-div stabilization and subgrid pressure models for the incompressible Navier-Stokes equations. *Comput. Methods Appl. Mech. Engrg.*, 198(49-52):3975–3988, 2009.

[27] Maxim A. Olshanskii and Arnold Reusken. Grad-div stabilization for Stokes equations. *Math. Comp.*, 73(248):1699–1718, 2004.

[28] Maxim A. Olshanskii, Andriy Sokolov, and Stefan Turek. Error analysis of a projection method for the Navier-Stokes equations with Coriolis force. *J. Math. Fluid Mech.*, 12(4):485–502, 2010.

[29] Jinshui Qin. *On the Convergence of Some Low Order Mixed Finite Elements for Incompressible Fluids*. PhD thesis, Department of Mathematics, Pennsylvania State University, 1994.

[30] L. R. Scott and M. Vogelius. Conforming finite element methods for incompressible and nearly incompressible continua. In *Large-scale computations in fluid mechanics, Part 2 (La Jolla, Calif., 1983)*, volume 22 of *Lectures in Appl. Math.*, pages 221–244. Amer. Math. Soc., Providence, RI, 1985.

[31] Chunjiang Shuai, Kaimin Teng, and Hongen Jia. On the error estimates of a new operator splitting scheme for the Navier-Stokes equations with Coriolis force. *Math. Probl. Eng.*, pages Art. ID 105735, 24, 2012.

[32] Andriy Sokolov. Analysis and numerical realisation of discrete projection methods for rotating incompressible flows. *PhD thesis, TU Dortmund, Germany,*, pages 485–502, 2008.

[33] Hai Yan Sun, Ling Yu Song, and Hong En Jia. Error analysis of the incremental pressure-correction projection scheme for the Navier-Stokes equations with Coriolis force. *Gongcheng Shuxue Xuebao*, 28(4):482–488, 2011.

[34] Shangyou Zhang. A new family of stable mixed finite elements for the 3D Stokes equations. *Math. Comp.*, 74(250):543–554, 2005.